Towards Zwitterionic Oligonucleotides with Improved Properties: the NAA/LNA-Gapmer Approach

Melissa Wojtyniak,[a] Boris Schmidtgall,[b] Philine Kirsch,[a] and Christian Ducho*[a, b]

In memory of Professor Thomas C. Bruice (1925–2019).

Oligonucleotides (ON) are promising therapeutic candidates, for instance by blocking endogenous mRNA (antisense mechanism). However, ON usually require structural modifications of the native nucleic acid backbone to ensure satisfying pharmacokinetic properties. One such strategy to design novel antisense oligonucleotides is to replace native phosphate diester units by positively charged artificial linkages, thus leading to (partially) zwitterionic backbone structures. Herein, we report a "gapmer" architecture comprised of one zwitterionic central segment ("gap") containing nucleosyl amino acid (NAA) modifications and two outer segments of locked nucleic acid (LNA). This NAA/LNA-gapmer approach furnished a partially zwitterionic ON with optimised properties: i) the formation of stable ON-RNA duplexes with base-pairing fidelity and superior target selectivity at 37 °C; and ii) excellent stability in complex biological media. Overall, the NAA/LNA-gapmer approach is thus established as a strategy to design partially zwitterionic ON for the future development of novel antisense agents.

Introduction

Oligonucleotides (ON) represent attractive candidates for novel therapeutic agents due to their unique binding mode, that is, hybridisation with complementary endogenous nucleic acids. Hence, they enable interference with protein biosynthesis through several modes of action: i) the antisense mechanism;[1] ii) the antigene mechanism;[2] and iii) the RNA interference mechanism.[3] These unique interaction pathways have already been proven to be clinically useful. For instance, fomivirsen, an antiviral antisense oligonucleotide used against cytomegalovirus retinitis, was approved by the FDA as the very first antisense drug on the market in 1998.[4a] In the following years, a few other ON were approved for clinical use, such as mipomersen for the treatment of familial hypercholesterolemia,[4b] nusinersen against spinal muscular atrophy[4c] and eteplirsen to treat Duchenne muscular dystrophy.[4d] However, the development of ON into pharmaceuticals is significantly hampered due to several characteristics of their phosphate diester backbone. First, its dense negative charge results in restrained cell permeability. Second, the native phosphate diester linkage is labile towards nuclease-mediated hydrolysis.

In order to overcome these hurdles, a large toolbox of various backbone modifications has been established over the past decades. According artificial backbone structures can be: i) the sole substitution of single atoms within the phosphate diester unit, for example, methylphosphonates[5] or the broadly used phosphorothioates;[6] ii) replacement of the phosphate diester with electroneutral groups, for instance with amides[7] or sulfones;[8] iii) a complete replacement of the native sugar-phosphate backbone, such as in peptide nucleic acids (PNA).[9]

Furthermore, modifications of the (2′-deoxy)ribose units can also furnish improved properties of ON analogues. For instance, Wengel and co-workers have developed unnatural locked nucleic acids (LNA) to alter the native ON characteristics (Figure 1A).[10] The LNA modification is characterised by an additional bridging bond, linking the 2′-oxygen of the ribose with the 4′-position, thus locking it in the 3′-*endo* conformation. Insertion of this rigid sugar significantly increases binding affinity towards RNA, due to a reduced entropic penalty upon hybridisation. In addition, the LNA modification was shown to significantly enhance stability against nuclease-mediated degradation, thereby improving the overall stability in biological media. As a result, LNA-modified ON have found pronounced attention as potential biomedical agents.[10c] Yet, the improved affinity for duplex formation was also shown to be accompanied by limited sensitivity towards base mismatches and thus, by decreased binding selectivity. Furthermore, the high melting temperatures of LNA-ON in complex with their RNA targets have been shown to be correlated to increased cytotoxicity resulting from elevated off-target effects, as well as increased hepatotoxic risks.[11a] To elucidate this toxic potential, Dieckmann et al. have developed an *in vitro* approach to evaluate the hybridisation-dependent toxicity of high-affinity ON, which confirmed a correlation of high melting temperatures (T_m values) and undesired toxic effects.[11b]

[a] M. Wojtyniak, P. Kirsch, Prof. Dr. C. Ducho
Department of Pharmacy, Pharmaceutical and Medicinal Chemistry, Saarland University
Campus C2 3, 66123 Saarbrücken (Germany)
E-mail: christian.ducho@uni-saarland.de
[b] Dr. B. Schmidtgall, Prof. Dr. C. Ducho
Department of Chemistry, University of Paderborn
Warburger Str. 100, 33098 Paderborn (Germany)

Supporting information for this article is available on the WWW under https://doi.org/10.1002/cbic.202000450

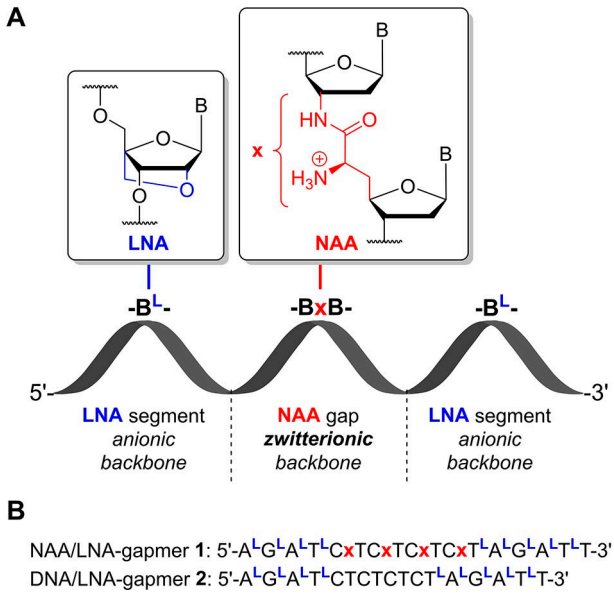

Figure 1. A) Schematic representation of the NAA/LNA-gapmer approach. B = nucleobase, ^{L} = LNA-modification, x = NAA-modification. B) Sequences of novel NAA/LNA-gapmer **1** and DNA/LNA-gapmer **2** (as reference ON). All unlabelled linkages are native phosphate diesters.

An alternative strategy in the development of backbone-modified ON involves the replacement of the anionic phosphate diester unit with artificial, positively charged linkers, thus creating an either partially zwitterionic[12] or fully cationic[13] ON. This approach significantly differs from the introduction of positive charges by modification of the 2′-hydroxy groups (in RNA) or nucleobases, while leaving the phosphate diester backbone unchanged. Such strategies also afford zwitterionic structures, but result in densely charged oligonucleotides.[14] In contrast, cationic replacements of the anionic phosphate diester enable the synthesis of artificial ON with a reduced net charge due to the compensation for adjacent phosphates. This substitution has been shown to have a positive effect on the ability to penetrate biological barriers such as cellular membranes.[15] So far, four suitable types of unnatural cationic linkers have been reported: i) Letsinger's phosphoramidate linkages[16] that carry a positively charged head group connected to the phosphate by an alkyl chain; ii) the guanidine[17] and iii) *S*-methylthiourea[18] modifications, both first described by Bruice et al.; and the iv) nucleosyl amino acid (NAA) modification (Figure 1A), an amide-derived cationic backbone motif previously reported by our group.[12,13b,c,19]

The NAA internucleoside structure has been formally derived from the "high-carbon" nucleoside core unit of naturally occurring muraymycin antibiotics and their synthetic analogues.[12,20] In terms of conformational flexibility, the NAA-linkage is somewhat intermediate to the rather flexible phosphoramidates and the rigid guanidines and *S*-methylthioureas. Its peptide-like structure features a primary amino group carrying a positive charge at physiological pH. This unit can be attached with a specific spatial orientation, that is, with stereoselectivity at the 6′-position of the adjacent "high-carbon" nucleoside.[12,13b,c] Partially zwitterionic ON including up to four NAA-modifications in an otherwise anionic (i.e., phosphate-based) backbone had previously been proven to form stable helical duplexes with complementary DNA. They were also shown to preserve excellent base-pairing fidelity, as demonstrated by decreasing melting temperatures due to base mismatches in the DNA counterstrand. For hybrid duplexes of NAA-containing DNA-ON with RNA, however, a fairly significant loss in thermal stability was observed (ΔT_m up to ~4.0 °C/modification). In this context, the 6′*S*-configured NAA linkage seemed to exert a slightly greater destabilising effect than the 6′*R*-configured congener.[12a] The biological *in vitro* evaluation of NAA-modified DNA-ON confirmed high stability against cleavage by 3′→5′- and 5′→3′-exonucleases as well as in more complex biological media (human plasma, whole cell lysate).[19]

For the future development of NAA-containing partially zwitterionic ON towards potential biomedical agents, one major issue was the undesired decrease in thermal stability for duplexes with complementary RNA strands (as these would represent the drug targets in antisense applications). Hence, we have envisioned to overcome this hurdle by using a "gapmer" approach,[21] that is, a hybrid structure with different internucleoside linkages in the middle of the ON than at its ends. The overall goal was to obtain a chimeric, partially zwitterionic NAA-containing ON that exerts high affinity towards its target RNA, while still showing excellent base-pairing fidelity. LNA units facilitate the formation of thermally highly stable DNA/RNA heteroduplexes (*vide supra*). Hence, it was planned to exploit this feature for the design of according NAA-containing gapmers. We have therefore designed a partially zwitterionic gapmer-ON consisting of LNA segments at the 3′- and the 5′-ends and a block of 6′*R*-configured NAA-modified DNA filling the "gap" in the central section (Figure 1A).

In this work, we report the synthesis of the novel NAA/LNA-gapmer **1** (with a partially zwitterionic backbone) and its properties in comparison with DNA/LNA-gapmer **2** (as a reference ON with a fully anionic backbone, Figure 1B). The identical base sequence of **1** and **2** has been artificially designed in order to study the fundamental principles of a zwitterionic gapmer construct such as **1**, that is, its sequence is not (yet) designed to target a specific biologically relevant RNA sequence. The choice of this sequence was based on synthetic considerations and the goal to obtain an ON containing all four canonical bases, while having a reasonable G-C content. The reported results strongly indicate that the NAA/LNA-gapmer approach is a useful strategy to design partially zwitterionic ON with improved properties.

Results

Synthesis of gapmer ON 1 and 2

It was envisioned to prepare both target ON **1** and **2** (Figure 1) by modified automated solid-phase-supported ON synthesis using phosphoramidite methodology. To synthesise the NAA/LNA-gapmer **1**, a "dimeric" CxT–NAA phosphoramidite (with

6′*R*-configuration in the NAA linkage) had to be prepared.[12] Thus, the aforementioned goal to obtain a gapmer ON with reasonable G-C content could be reached, as the only previously reported "dimeric" NAA phosphoramidites had been TxT[12a] and AxT,[12b] respectively (with "x" representing the NAA linkage, cf. Figure 1). The synthesis of this novel CxT-NAA phosphoramidite required the preparation of a suitably protected 3′-amino-2′,3′-dideoxycytidine building block (Scheme 1). Different synthetic routes towards such a 3′-aminodeoxycytidine building block had been described before.[22] With respect to its elegance and high stereoselectivity, our synthetic strategy was mainly based on the procedure reported by Richert and coworkers.[22d]

Thus, 2′-deoxycytidine **3** was *N*-benzoylated at the nucleobase using a standard transient protection protocol,[23] furnishing *N*-benzoyl-2′-deoxycytidine **4** in 96% yield (Scheme 1). In contrast to the recrystallisation procedure described by Ti et al., compound **4** was purified by column chromatography to remove excess benzoic acid. This was followed by a sequence of two Mitsunobu reactions, with the first one leading to 5′-(*p*-bromobenzoyl) protection and the second one enabling ring closure of the cytosin-2-O and C-3′, to give cyclised product **5** in 39% yield. Nucleophilic substitution (S_N2) at C-3′ with sodium azide then furnished 3′-azidonucleoside **6** in 66% yield. After saponification of the *p*-bromobenzoyl ester, silylation gave 5′-*O*-TBDMS-protected derivative **7** in 85% yield over two steps from **6**. Finally, reduction of the azido group by transfer hydrogenation[24] afforded the desired protected 3′-amino-2′,3′-dideoxycytidine derivative **8** in 96% yield (Scheme 1).

Based on our stereoselective route for the synthesis of uridine-derived nucleosyl amino acids,[25] we had previously developed the preparation of according thymidine derivatives.[12,13b] Hence, this reported protocol was used to prepare protected nucleosyl amino acid **9** (Scheme 2, reactions not shown).[12] Thymidine derivative **9** underwent amide coupling with 3′-aminonucleoside **8** to furnish the bis-silylated NAA-linked C-T dimer **10** in 78% yield. Fluoride-mediated desilylation gave diol **11** in a moderate yield of 53%. Attempts to improve this deprotection protocol for the TBDMS ethers were not successful, as changes in the reaction conditions always led to more side reactions or even complete decomposition of starting material **10**. Regioselective 5′-*O*-dimethoxytritylation afforded 5′-*O*-DMTr-protected NAA-linked dimer **12** (64% yield), which was then phosphitylated (using diamidite reagent **13**) to give the dimeric NAA-linked C-T phosphoramidite **14** in 78% yield (Scheme 2).

With the NAA-linked C-T phosphoramidite **14** in hand, both gapmers **1** and **2** (Figure 1) were assembled on the DNA synthesiser. Standard protocols were slightly adjusted (see the Supporting Information for details). In general, coupling times for LNA and NAA phosphoramidites were prolonged relative to their commercially available, unmodified DNA congeners, and the number of couplings was increased to enhance the step-to-step yield. With respect to the activator for phosphoramidite coupling, it was found that benzylmercaptotetrazole (BMT) was superior to 4,5-dicyanoimidazole (DCI) as it gave higher yields, in particular when the NAA-linked building block **14** was coupled. Apart from this, standard solvents and reagents for solid-phase-supported DNA synthesis and the usual basic work-up procedure were used. Purification of gapmers **1** and **2** was achieved by polyacrylamide gel electrophoresis (PAGE) with urea as chaotropic component. The identities of gapmers ON **1** and **2** were confirmed by high resolution mass spectrometry (see the Supporting Information).

NAA/LNA-gapmer 1 shows superior hybridisation properties at physiologically relevant temperature

One main goal of the reported gapmer approach was to enhance the stability of NAA-containing DNA-RNA hybrid duplexes, while retaining base-pairing fidelity. Therefore, melting temperature experiments with fully complementary strands as well as with mismatched RNA-ON **X** (base mismatch opposite of one of the LNA segments: 5′-AAUCUAGAGAGAGA**C**CU-3′) and mismatched RNA-ON **Y** (base mismatch opposite of the

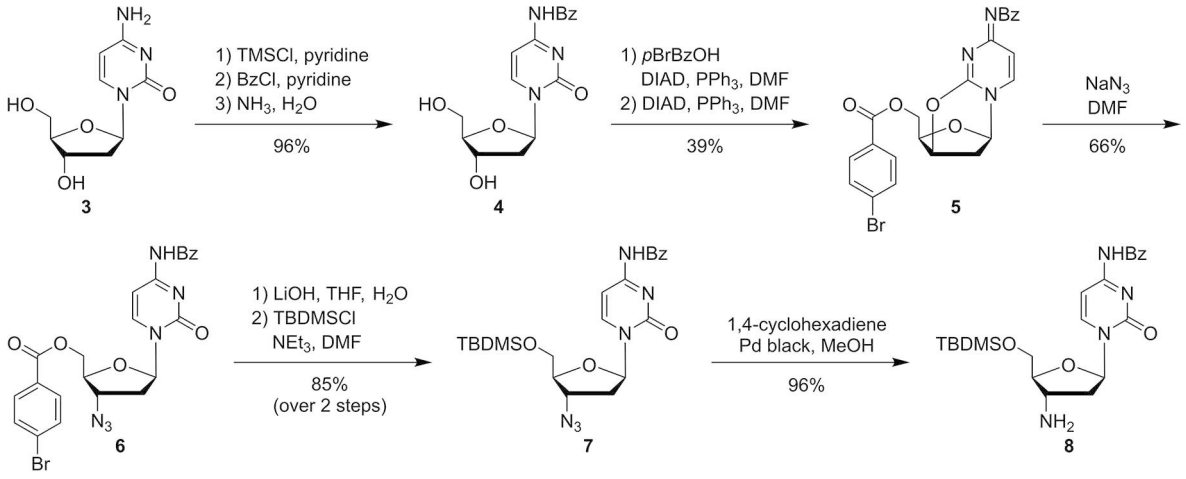

Scheme 1. Synthesis of the protected 3′-amino-2′,3′-dideoxycytidine building block **8**.

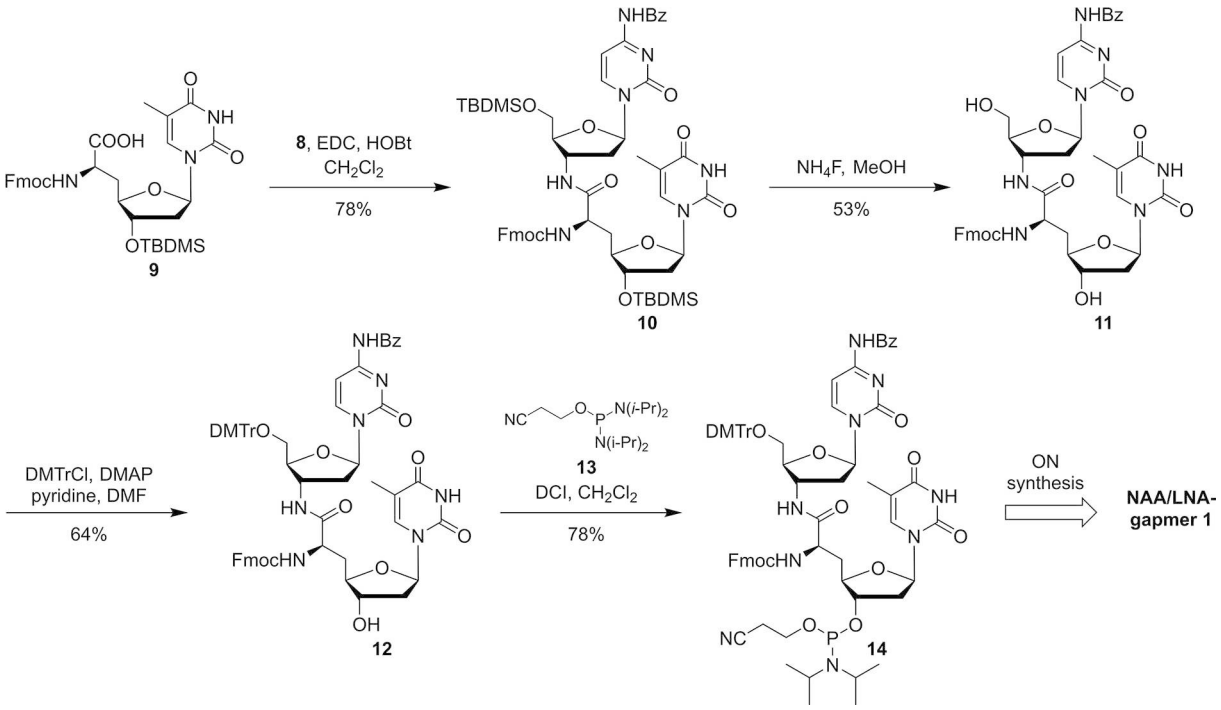

Scheme 2. Synthesis of the "dimeric" NAA-linked C–T phosphoramidite **14** for automated ON synthesis.

central NAA gap: 5′-AAUCUAGAG**G**GAGAUCU-3′) were performed. To eliminate the temperature dependency of the extinction coefficient ε, αT_m values were calculated and used to describe the melting temperature of all studied duplexes. Furthermore, $\alpha T_{37^\circ C}$ values were calculated to investigate the hybridisation at a physiologically relevant temperature of 37 °C (for more details see the Supporting Information). The obtained results are given in Table 1, with selected melting curves shown in Figure 2.

Satisfactorily, the duplex stability of the NAA/LNA-gapmer **1** (Figure 1) with fully complementary DNA was equal to the according native DNA/DNA duplex ($\alpha T_m = 48.5$ °C, entries 9 vs. 1, Table 1), whereas control gapmer **2** furnished an even higher value ($\Delta\alpha T_m = +4.5$ °C, entry 5). This was also the case for the **2**-RNA duplex, for which an even stronger increase in melting temperature was observed ($\Delta\alpha T_m = +17.0$ °C, entry 6). This was anticipated as the LNA segments in gapmer **2** were supposed to stabilise duplexes with native RNA.[10] However, for the hybridisation of the complementary RNA strand with NAA-

Table 1. αT_m values [°C] of native DNA (entries 1–4), DNA/LNA-gapmer **2** (entries 5–8) and NAA/LNA-gapmer **1** (entries 9–12) in complex with either complementary DNA, complementary RNA, mismatched RNA **X**, and mismatched RNA **Y**, respectively. ^{L} = LNA modification, **x** = NAA modification (Figure 1). All unlabelled linkages are native phosphate diesters. Mismatches in RNA-ON **X** and **Y** are highlighted in bold and underlined.

NAA/LNA-gapmer **1**: 5'-A^{L}G^{L}A^{L}T^{L}C**x**TC**x**TC**x**T^{L}A^{L}G^{L}A^{L}T^{L}T-3' **X**: 5'-AAUCUAGAGAGAGA**C**CU-3'
DNA/LNA-gapmer **2**: 5'-A^{L}G^{L}A^{L}T^{L}CTCTCTCT^{L}A^{L}G^{L}A^{L}T^{L}T-3' **Y**: 5'-AAUCUAGAG**G**GAGAUCU-3'

	Duplex	αT_m [°C]	$\Delta\alpha T_m$ [°C][a]	$\alpha T_{37^\circ C}$	$\alpha T_{37^\circ C}$ [%]	$1-\alpha T_{37^\circ C}$ [%]
1	DNA + DNA	48.5	–	0.97	97	3
2	DNA + RNA	55.5	–	1.00	100	0
3	DNA + **X**	50.0	–	0.97	97	3
4	DNA + **Y**	52.0	–	0.98	98	2
5	gapmer **2** + DNA	53.0	4.5	0.98	98	2
6	gapmer **2** + RNA	72.5	17.0	1.00	100	0
7	gapmer **2** + **X**	62.5	12.5	1.00	100	0
8	gapmer **2** + **Y**	68.5	16.5	1.01	100	0
9	gapmer **1** + DNA	48.5	0.0	0.96	96	4
10	gapmer **1** + RNA	49.5	−6.0	0.98	98	2
11	gapmer **1** + **X**	37.0	−13.0	0.51	51	49
12	gapmer **1** + **Y**	43.0	−9.0	0.86	86	14

[a] $\Delta\alpha T_m$ values were calculated based on the difference to native duplexes, i.e., αT_m (gapmer + counterstrand) − αT_m (native DNA + counterstrand).

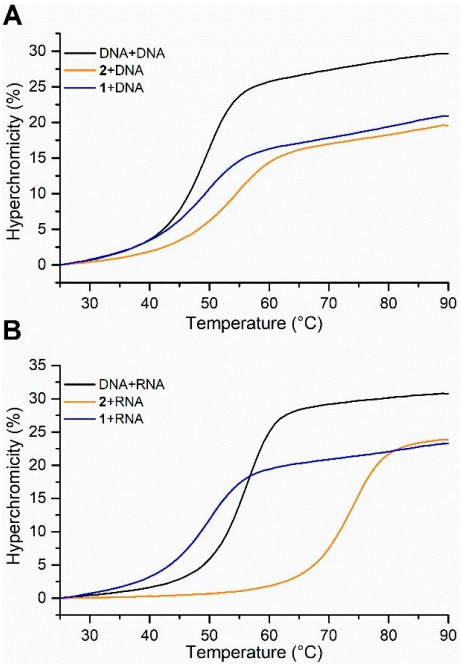

Figure 2. A) Melting curves of native DNA, DNA/LNA-gapmer **2**, and NAA/LNA-gapmer **1** in complex with complementary DNA. B) Melting curves of native DNA, DNA/LNA-gapmer **2**, and NAA/LNA-gapmer **1** in complex with complementary RNA. All depicted curves are the average of technical triplicates.

containing gapmer **1**, this overall stabilising effect was not found. Instead, a slight decrease in the melting temperature was observed ($\Delta\alpha T_m = -6.0\,^{\circ}C$, entry 10). This decrease in duplex stability is equivalent to about $-5.8\,^{\circ}C$ per NAA modification (entry 10 vs. entry 6), which is similar to the previously described destabilising effect of the NAA modification on DNA-RNA hybrid duplexes (~3.5 °C per NAA modification for a comparable type of sequence).[12a] The presence of the stabilising LNA units then limits the overall destabilisation of the **1**-RNA duplex to a formal value of $-1.5\,^{\circ}C$ per NAA modification (entry 10 vs. entry 2). Therefore, the results obtained with ON **1** demonstrated that the gapmer architecture with two flanking LNA segments indeed furnished an improved duplex stability for hybridisation with RNA.

For a more detailed analysis of the hybridisation properties of gapmer **1**, we considered the overall ratio of hybrid duplex to free single strands at physiological human body temperature (37 °C), as this property is decisive for any potential *in vivo* application of antisense ON. Thus, the *y* values of the α-curve for $T = 37\,^{\circ}C$ were determined for every thermal denaturation experiment ($\alpha T_{37^{\circ}C}$ values, Table 1, see also the Supporting Information for the exact procedure). These values correspond to the amount of duplex present at this given temperature and can therefore also be expressed as a percentage of hybridised (i.e., bound) ON ($\alpha T_{37^{\circ}C}$ values in %). Correspondingly, the term $1-\alpha T_{37^{\circ}C}$ provides the unbound, single-stranded ON fraction (Table 1). It was found that hybridisation of native DNA and RNA of the given sequence occurred with 100% at 37 °C (entry 2, Table 1). This was also the case for the mixture of reference gapmer **2** and complementary RNA under these conditions (entry 6). For the NAA/LNA-gapmer **1** and complementary RNA, almost quantitative (98%) hybridisation at 37 °C was determined, with only ~2% single-stranded fraction (entry 10). This demonstrated the possibility to achieve excellent target engagement by such an NAA-containing gapmer under physiologically relevant conditions.

We then studied the base-pairing fidelity of NAA/LNA-gapmer **1**, that is, its hybridisation properties with RNA-ON containing a single base mismatch. Therefore, gapmer **1** as well as both reference ON (**2** and native DNA, respectively) were investigated for duplex formation with two different mismatched RNA-ON: i) the aforementioned RNA strand **X** having a mismatching base opposite one of the LNA segments of **1**; ii) the aforementioned RNA strand **Y** having the mismatch opposite the zwitterionic NAA-modified gap of **1**. In all resultant cases (i.e., with gapmers **1** and **2** as well as with native DNA), a decrease in thermal duplex stability due to the introduction of base mismatches was observed (entries 3 and 4 vs. entry 2; entries 7 and 8 vs. entry 6; entries 11 and 12 vs. entry 10, Table 1; also see Figure S7 in the Supporting Information). Furthermore, in all of these experiments, the mismatch-mediated destabilisation of duplex structures was most pronounced when the mismatched base was placed opposite the LNA segment, that is, with RNA-ON **X** as counterstrand (entries 3, 7, and 11). Interestingly, NAA/LNA-gapmer **1** proved to be highly sensitive towards both mismatched RNA-ON **X** and **Y** (entries 11 and 12 vs. entry 10). In this case, mismatch recognition was found to be even better than for the native DNA strand (entries 3 and 4 vs. entry 2), as expressed by a stronger mismatch-induced destabilisation of the duplex structures. Again, the duplex-to-single strand ratio at 37 °C was determined from the melting curve data (*vide supra*). Both reference ON (gapmer **2** and native DNA) showed a large percentage of duplex structures at 37 °C ($\alpha T_{37^{\circ}C} = 97$–$100\%$), both with **X** and **Y** as counterstrands (entries 3, 4, 7, and 8). Only the NAA/LNA-gapmer **1** was partially dissociated from the mismatched RNA-ON under these conditions (entries 11 and 12). In the presence of **Y**, 14% of gapmer **1** was not bound to the RNA-ON, and with **X**, the unbound fraction of the gapmer was even ~50%. This selectivity in RNA binding led to the conclusion that the hybridisation properties of NAA/LNA-gapmer **1** are superior relative to both the reference gapmer **2** and to native DNA (*vide infra*), even though the presence of the NAA-modification furnished a moderate decrease of thermal duplex stability.

Circular dichroism spectra of both gapmers in complex with DNA or RNA demonstrate structural resemblance to a DNA-RNA heteroduplex

In order to elucidate the structural properties of the partially zwitterionic NAA/LNA-gapmer **1**, circular dichroism (CD) spectra of duplexes of **1** either with complementary DNA (Figure 3A) or RNA (Figure 3B) were recorded and compared to the respective

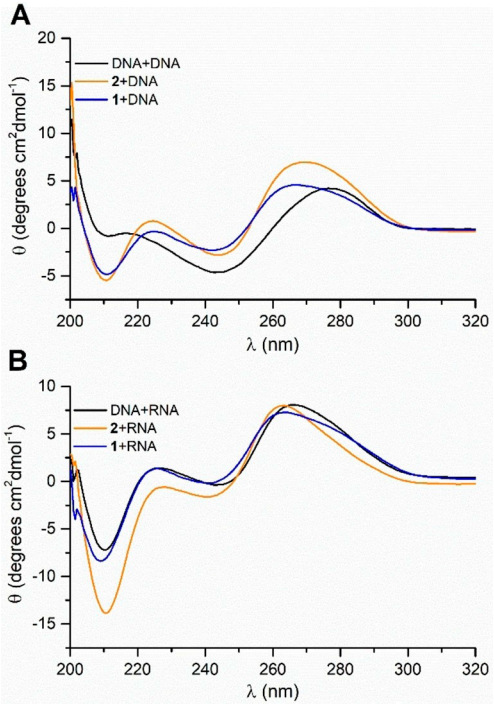

Figure 3. CD spectra of native DNA, DNA/LNA-gapmer **2**, and NAA/LNA-gapmer **1** in complex with complementary A) DNA and B) RNA. All depicted curves are the average of technical triplicates.

spectra of DNA/LNA-gapmer **2** with complementary counterstrands.

For the duplexes of either gapmers **1** or **2** with DNA, CD signals indicated more resemblance between both gapmer-containing duplexes than to the unmodified DNA–DNA duplex of the same sequence (Figure 3A). In particular regarding the distinct negative signal at 210 nm and the following positive amplitude at 225 nm – which were almost nonexistent for the DNA-DNA reference duplex – duplexes containing gapmers **1** and **2** showed pronounced similarities. This hints towards substantial structural differences in the conformation of both gapmer-DNA duplexes as compared to the native DNA-DNA helix. However, when according duplexes with a complementary RNA counterstrand were studied, striking similarities to the unmodified DNA-RNA congener were observed (Figure 3B). In this case, the CD signals of the **1**-RNA duplex almost perfectly superposed with the native DNA-RNA duplex. This was also the case for reference gapmer **2**, with the slight difference that the negative signal at 210 nm was stronger than for the other two duplexes. Furthermore, the CD spectra of the **1**-RNA and **2**-RNA duplexes show some resemblance to the spectra of the **1**-DNA and **2**-DNA congeners, respectively (Figure 3B vs. A). Overall, these results therefore demonstrate that both gapmers **1** and **2**, either in complex with DNA or RNA, furnish duplexes with topologies similar to a DNA-RNA heteroduplex. Remarkably, this finding was independent of the charge pattern in the ON backbone, that is, the partially zwitterionic nature of gapmer **1**.

Both gapmer ON show excellent stability in biological media

Stability in biological media is crucial for any potential *in vivo* application of antisense ON. Therefore, we tested the stability of both gapmers **1** and **2** in pooled human plasma (HP; Figure 4A) as well as in whole cell lysate (WCL) of the human U937 cell line (Figure 4B). Unmodified DNA served as the positive (i.e., degradable) control in both assays.

We had previously reported that NAA-modified ON have potentially excellent stabilities in such media, dependent on the position of the cationic NAA-linkage.[19] LNA-modified ON are also known to show an improved stability against nuclease-mediated degradation[26a] and also in human serum, relative to unmodified controls.[26b] In this work, we have aimed to verify the thus anticipated stability of gapmers **1** and **2** in the aforementioned biological media. Analysis by urea-PAGE demonstrated that both gapmers **1** and **2** show excellent stability against cleavage in HP (Figure 4A) as well as in WCL (Figure 4B) over a time course of eight hours, whereas an unmodified DNA-ON of the same sequence was completely cleaved.

Duplex formation of NAA/LNA-gapmer 1 with complementary RNA results in moderate activation of RNase H

In order to determine whether NAA/LNA-gapmer **1** is capable of triggering RNase H-mediated cleavage of complementary RNA, an assay employing a 5′-^{32}P-labelled RNA strand was used.[27] Duplexes of native DNA as well as of DNA/LNA-gapmer **2**, respectively, with this RNA strand served as controls, with the

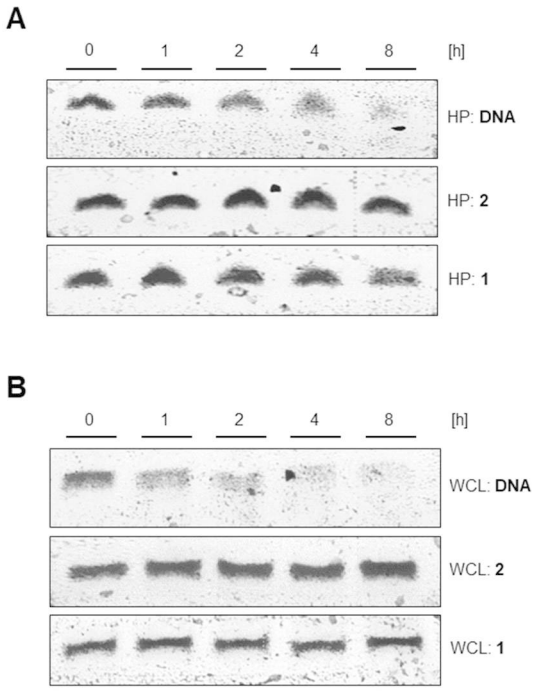

Figure 4. Effect of A) human plasma (HP) and B) human whole-cell lysate (WCL) on native DNA as well as on gapmers **1** and **2**, respectively, over a time course of eight hours (analysis by urea-PAGE).

DNA-RNA heteroduplex representing a positive control, that is, a system furnishing RNase H-catalysed RNA degradation.

Figure 5A shows the results of the incubation of the labelled RNA with all three aforementioned strands, respectively, and RNase H over a time course of 60 min. Furthermore, the bottom panel depicts the influence of RNase H on the ^{32}P-labelled RNA strand without the presence of any counterstrand as an additional control experiment. Analyses of the assay mixtures were carried out by urea-PAGE and autoradiography. As anticipated,[28] DNA/LNA-gapmer **2** induced the activation of RNase H and led to complete degradation of the parent RNA strand within the first 5 min of incubation (Figure 5A, degradation product label **b**). The timepoint of 0 min shows the intact RNA (Figure 5A, label **a**) as well as a band of the **2**-RNA duplex (label **x**) which was still present despite the addition of urea as chaotropic agent. Similar observations were made for unmodified DNA that likewise triggered rapid degradation after 5 min, but led to the formation of an additional degradation product. In contrast, single-stranded RNA without a complementary counterstrand remained stable against RNase H over the observed timeframe. Interestingly, NAA/LNA-gapmer **1** also induced RNase H-mediated cleavage of the target RNA, although no uniform phosphate diester backbone was present in its structure. However, the rate of degradation appeared to be significantly slower than for reference gapmer **2**.

We therefore performed a second set of experiments to observe RNase H-mediated degradation over an extended time period (Figure 5B). After 24 h, degradation of the labelled RNA was clearly detectable in the assay mixture containing NAA/LNA-gapmer **1**, yet nearly the exact same outcome was observed without the presence of **1**. To rule out general instability of the chosen RNA sequence over such an extended time period, another control experiment was included: ^{32}P-labelled RNA was incubated over the full time period (i.e., up to 24 h) in the absence of both a counterstrand and RNase H. However, no RNA cleavage was detected under these conditions (Figure 5B). It has to be noted that the degradation signals observed for the duplex of **1** and ^{32}P-labelled RNA after 30 and 60 min (Figure 5A) could not be visualised in the prolonged incubation experiment (Figure 5B) due to differences in signal intensity.

Discussion

In previous studies,[12a,19] we reported the generally favourable properties of ON with partially zwitterionic NAA-modified backbone structures, that is, their formation of stable, helical duplexes with complementary DNA, their retention of base-pairing fidelity and their high stability in biological media. However, duplex formation with RNA had been observed to be moderately hampered, that is, decreased thermal stabilities (up to −4.0 °C/NAA-modification[12a]) had been observed. Thus, we have now aspired to modify such zwitterionic NAA-ON in a way that furnishes satisfactory binding affinity towards RNA without compromising base-pairing fidelity, hence potentially enabling an efficient and selective target engagement with endogenous RNA. These considerations have led to the design of NAA/LNA-gapmer **1**, in which strongly RNA-binding LNA segments were combined with a zwitterionic NAA-modified gap unit.

Following the successful synthesis of **1** (and an according DNA/LNA-gapmer **2** as a reference with a uniformly anionic backbone), UV-monitored thermal melting studies revealed an improved binding affinity to complementary RNA, relative to previously studied NAA-modified ON (formally −1.5 °C/NAA-modification due to the stabilising effect of the LNA units). As a

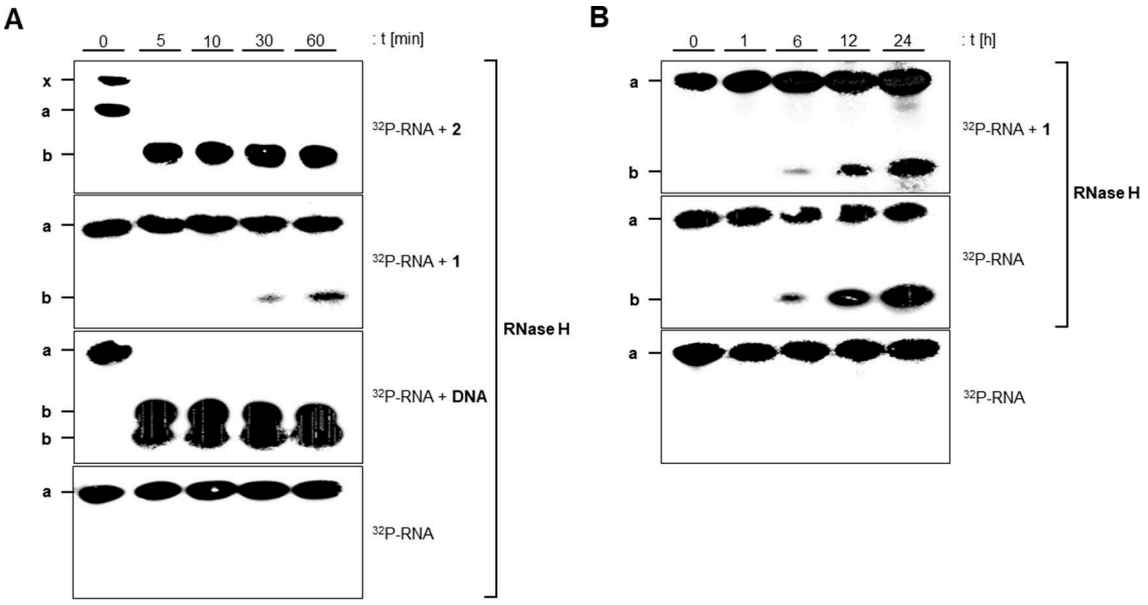

Figure 5. A) RNase H-mediated degradation of ^{32}P-labelled RNA upon hybridisation with **1**, **2**, native DNA, and without any counterstrand over 60 min (urea-PAGE). B) RNase H-mediated degradation of ^{32}P-labelled RNA with **1**, without any counterstrand, and without either counterstrand or RNase H over 24 h (urea-PAGE). **x**: heteroduplex of **2** and RNA, **a**: intact RNA, **b**: RNA degradation products.

result, almost quantitative formation of the **1**-RNA duplex at physiologically relevant 37 °C could be demonstrated. Furthermore, gapmer **1** was shown to be sensitive towards single base mismatches in the counterstrand at 37 °C. Experiments with mismatched RNA **X** resulted in only 50% formation of the **1**-RNA duplex at this temperature. With a different mismatched RNA **Y**, 14% single-stranded gapmer **1** was determined (cf. Table 1). Interestingly, this selectivity was not observed with the DNA/LNA-gapmer **2** (i.e., the polyanionic reference ON) that showed no sensitivity towards base mismatches in the RNA counterstrand at 37 °C. The same was true for unmodified DNA. Binding to RNA off-targets with sequences similar to the actual target mRNA can lead to potential side effects in the pharmaceutical application of antisense ON.[29] It is therefore of great relevance that backbone-modified ON structures show some sequence selectivity in their hybridisation properties under physiologically relevant conditions (i.e., at 37 °C). With respect to this consideration, the hybridisation properties of NAA/LNA-gapmer **1** are superior relative to those of both the reference gapmer **2** and native DNA, even though the presence of the NAA-modification furnished a decrease of thermal duplex stability. Furthermore, these results give rise to the general question if T_m values might be overrated in the evaluation of hybridisation properties of backbone-modified ON with respect to their potential application as antisense agents. We present herein an alternative parameter for such an evaluation: the target selectivity of the investigated ON (with a suitable length for an antisense agent) at 37 °C. This appears to be superior to a "the more stable, the better" approach for studying the physicochemical hybridisation properties with RNA counterstrands. This hypothesis is also supported by recent findings by Dieckmann et al. who could demonstrate a direct correlation of high T_m values and the hepatotoxic potential of high-affinity ON due to enhanced off-target effects.[11b] Of course, such an improved target selectivity due to decreased duplex stability can in principle also be achieved by alternative means, for example, designing a shorter sequence of the antisense ON or a lower number of LNA units. However, herein we demonstrate that the NAA-modification is a useful addition to the toolbox of ON modifications to achieve this goal.

CD-spectroscopic analyses confirmed helical topologies for the gapmers **1** and **2**, respectively, in complex with complementary DNA or RNA, with the resultant helical structures being similar to a DNA-RNA heteroduplex in all cases. This uniform topological preference was obviously caused by the presence of the LNA segments in the gapmer sequences.[30] Notably, the partially zwitterionic backbone structure of **1** had no distorting influence on the topologies of its duplexes formed with either DNA or RNA counterstrands. In addition, high stability against degradation of the gapmers in human plasma and whole cell lysate was observed.

The activation of RNase H generally represents a desirable (though not essential feature) of antisense ON, and the NAA/LNA-gapmer **1** was therefore investigated with respect to this property. In a first set of experiments, the RNase H-mediated cleavage of a complementary ^{32}P-labelled RNA counterstrand was studied over a period of 60 min. Within this time, the two reference ON (i.e., gapmer **2** and unmodified DNA) both induced rapid degradation of the target RNA by RNase H. Surprisingly, some degradation of the labelled RNA (albeit rather slowly) was also detected in presence of NAA/LNA-gapmer **1**, although **1** possesses no uniform phosphate diester backbone (cf. Figure 5). This suggested a very moderate activation of RNase H due to the presence of **1** in the assay mixture. In order to further study this effect, the assay was then performed again with a significantly extended incubation period (up to 24 h). Even though this led to stronger signals for the RNA degradation products with gapmer **1**, this result could not solely be linked to the influence of the partially zwitterionic gapmer: the same experimental setup with the absence of **1** resulted in a rather similar outcome. To exclude a general instability of the radiolabelled RNA strand, an additional control containing only the target RNA without RNase H was also incubated for 24 h, but no degradation was recorded. This demonstrated that the employed preparation of RNase H displayed some sort of unspecific nuclease activity. Overall, it was concluded that the aforementioned very moderate activation of RNase H by gapmer **1** became indistinguishable from background reactions over longer incubation periods. This suggests that an NAA/LNA-gapmer of type **1** might exert a potential antisense effect by "steric block" (i.e., binding to endogenous RNA) rather than by "catalytic" RNA degradation, as the latter would probably require a more efficient activation of RNase H. It should also be noted that this part of the reported work generally proves the high relevance of a rigorous set of control experiments in RNase H assays. Otherwise, it is unclear if the described alleged activation of RNase H was genuine or actually resulted (at least partially) from unspecific nuclease activity. This actually might be the case for several reports on 'RNAse H activation' by modified ON structures in the literature.

Conclusion

In summary, we report the synthesis and properties of a new type of gapmer oligonucleotide architecture featuring a partially zwitterionic backbone structure. This NAA/LNA-gapmer approach furnished a zwitterionic ON **1** with optimised characteristics: gapmer **1** showed superior hybridisation properties with RNA at physiologically relevant 37 °C as well as excellent stability in biological media. In a cellular setting, a gapmer of type **1** might then mainly exert biological activity via a 'steric block' mechanism, even though **1** apparently activated RNase H-mediated RNA degradation on a very moderate level. Overall, the NAA/LNA-gapmer approach is thus established as a strategy to design partially zwitterionic ON for the future development of novel antisense agents with a reduced overall charge in the backbone. This is anticipated to furnish improved pharmacokinetic properties of according ON-based drug candidates. Based on the favourable characteristics of **1**, the stage is now set for the development of synthetic methodology for the efficient preparation of zwitterionic gapmers of type **1** with biologically relevant base sequences. This will enable future

studies on their antisense efficacy *in cellulo*, with the goal to establish zwitterionic backbone architectures of oligonucleotide analogues as a viable strategy for the development of novel antisense agents.

Experimental Section

Synthesis of oligonucleotides: Based on our previous syntheses of NAA-modified ON,[12] gapmer ON **1** and **2** were assembled by automated solid phase-supported DNA synthesis. This required the chemical synthesis of "dimeric" NAA-linked phosphoramidite **14** (see the Supporting Information for detailed synthetic procedures). Unmodified DNA phosphoramidites (Glen Research) and LNA phosphoramidites (QIAGEN) were commercially purchased. After completion of ON synthesis and basic workup under standard conditions, purification of **1** and **2** was achieved by urea polyacrylamide gel electrophoresis (urea-PAGE, Figure S1, see the Supporting Information for detailed procedures). The identities of both gapmers **1** and **2** were confirmed by high resolution mass spectrometry (Table S1, Figures S2 and S3). All other oligonucleotides were commercially purchased (Sigma-Aldrich).

Melting temperature experiments: To determine the binding affinity of the NAA/LNA-gapmer **1** towards complementary DNA (5′-AATCTAGAGAGAGATCT-3′) and RNA (5′-AAUCUAGAGAGAGAUCU-3′), a 1 μM solution of the gapmer/counterstrand duplex in phosphate buffer (10 mM NaH_2PO_4, pH 7.4, containing 100 mM NaCl) was prepared. Prior to measurements, the solution was heated to 90 °C and subsequently cooled down to RT to enable duplex formation. Then, three heating and cooling cycles ranging from 25 to 90 °C with a heating rate of 0.7 °C/min were performed and changes in the absorption at $\lambda = 260$ nm were recorded using a Cary 100 UV/Vis spectrometer (Agilent Technologies). Hyperchromicity was plotted against temperature to obtain melting curves, and T_m values were calculated as the maximum of the first derivative. To eliminate the temperature dependency of the extinction coefficient ε, αT_m values were calculated and used to describe the melting temperature of all studied duplexes. Furthermore, $\alpha T_{37^\circ C}$ values were calculated to investigate the hybridisation at a physiologically relevant temperature of 37 °C. Details on the method for the compilation of the α-curves are provided in the Supporting Information (Figures S4 to S6). A similar protocol was used for studies on mismatch sensitivity. Therefore, base mismatches were introduced in the RNA counterstrand opposite of either one of the LNA segment (5′-AAUCUAGAGAGAGA**C**CU-3′, mismatched RNA-ON **X**) or the NAA gap (5′-AAUCUAGAG**G**GAGAUCU-3′, mismatched RNA-ON **Y**, mismatches are highlighted in bold and are underlined in the sequences, also see Figure S7). To obtain reference T_m values, according melting temperature experiments were conducted with DNA/LNA-gapmer **2** and a native DNA-ON with the same sequence (5′-AGATCTCTCTCTAGATT-3′).

CD-spectroscopic analysis of duplex structures: Circular dichroism (CD) spectra of duplexes containing the NAA/LNA-gapmer **1** were recorded in phosphate buffer (10 mM NaH_2PO_4, pH 7.4, containing 100 mM NaCl) on a Jasco 715 spectropolarimeter. The final concentration of the duplex was 1 μM. All measurements were performed at 25 °C in a cuvette with a length of 1 cm and a wavelength range of 200–320 nm. Every sample was scanned 10 times with a scanning speed of 200 nm/min, a bandwidth of 5 nm, response time of 2 s and a data pitch of 0.5 nm. Prior to data analysis, a background correction was performed. Spectra were obtained by plotting the mean residual ellipticity Θ against the recording wavelength λ. Reference spectra were recorded using the same protocol and duplexes containing either the DNA/LNA-gapmer **2** or a native DNA-ON with the same sequence (5′-AGATCTCTCTCTAGATT-3′).

Stability assays in biological media: The stabilities of both gapmer ON **1** and **2** in biological media was studied using pooled human plasma and whole-cell lysate of the U937 cell line as described before.[19] As a positive control for the degradation of ON in these media, a native DNA-ON with the same sequence (5′-AGATCTCTCTCTAGATT-3′) was used. In contrast to the previously reported protocol,[19] incubation times for both ON were increased to a total of 8 h. Samples were taken at the time points shown in Figure 4 (*vide supra*). Pooled human plasma was obtained from BIOTREND Chemikalien GmbH. U937 cells were purchased from Sigma-Aldrich and the whole-cell lysate was prepared as reported.[19]

RNase H assays: An RNA-ON with a sequence (5′-AAUCUAGAGAGAGAUCU-3′) complementary to the gapmer sequence was radiolabelled at the 5′-end using γ-^{32}P-ATP (Hartmann Analytics, 500 μCi). The phosphorylation reaction was catalysed by T4 polynucleotide kinase according to the manufacturer's protocol (kit for DNA/RNA 5′-end labelling, Thermo Scientific). The resultant 5′-radiolabelled RNA was purified on an illustra NAP-5 gravity flow column (GE Healthcare) using water (Milli-Q) as eluent. The solvent was evaporated under reduced pressure and the dry 5′-^{32}P-labelled RNA was redissolved in water to a final concentration of 10 μM. The labelled RNA (2.5 pmol) was then combined with the NAA/LNA-gapmer **1** (5 pmol), diluted with 10x Reaction Buffer (Thermo Scientific) to a total volume of 25 μL and incubated at 37 °C for 15 min to allow formation of the hybrid duplex. Subsequently, RNase H from *E. coli* MRE-600 cells (Thermo Scientific, 1 μL, 10 U) was added and the mixture was incubated at 37 °C. Samples were taken at the time points shown in Figure 5 (*vide supra*) and the reaction was quenched by addition of stop-mix (50 mM EDTA, 90% formamide, 5 mg bromophenol blue). The resultant final samples were analysed on a urea-PAGE gel[19] and bands were visualised using a Typhoon 9410 phosphoimager (GE Healthcare, Figure 5). DNA/LNA-gapmer **2** and a native DNA-ON with the same sequence (5′-AGATCTCTCTCTAGATT-3′) were used as positive controls. Furthermore, two negative controls were included: i) incubation under the conditions described above, but lacking the gapmer strand, to determine the influence of the activating strand; ii) incubation under the conditions described above, but lacking both the gapmer strand and RNase H, to elucidate potential unspecific RNase activity of the RNase H preparation.

Acknowledgements

We thank the Deutsche Forschungsgemeinschaft (DFG, grant DU 1095/2-1), the Fonds der Chemischen Industrie (FCI, Sachkostenzuschuss) and the Studienstiftung des deutschen Volkes (doctoral fellowship for B.S.) for financial support. Open access funding enabled and organized by Projekt DEAL.

Conflict of Interest

The authors declare no conflict of interest.

Keywords: antisense · backbone modification · gapmers · oligonucleotides · zwitterions

[1] a) X. Shen, D. R. Corey, *Nucleic Acids Res.* **2018**, *46*, 1584–1600; b) C. F. Bennett, *Annu. Rev. Med.* **2019**, *70*, 307–321.
[2] a) B. A. Armitage, *Nat. Chem. Biol.* **2005**, *1*, 185–186; b) V. K. Sharma, P. Rungta, A. K. Prasad, *RSC Adv.* **2014**, *4*, 16618–16631.
[3] a) Y. Dong, D. J. Siegwart, D. G. Anderson, *Adv. Drug Delivery Rev.* **2019**, *144*, 133–147; b) M. Caillaud, M. El Madani, L. Massaad-Massade, *J. Controlled Release* **2020**, *321*, 616–628.
[4] a) J. Temsamani, G. S. Pari, P. Guinot, *Expert Opin. Invest. Drugs* **1997**, *9*, 1157–67; b) J. S. Parham, A. C. Goldberg, *Expert Opin. Pharmacother.* **2019**, *2*, 127–131; c) K. Goodkey, T. Aslesh, R. Maruyama, T. Yokota, *Methods Mol. Biol.* **2018**, 69–76; d) M. Rodrigues, T. Yokota, *Methods Mol. Biol.* **2018**, 31–55.
[5] P. S. Miller, J. Yano, E. Yano, C. Carroll, K. Jayaraman, P. O. P. Ts'o, *Biochemistry* **1979**, *18*, 5134–5143.
[6] F. Eckstein, *Annu. Rev. Biochem.* **1985**, *54*, 367–402.
[7] a) J. Lebreton, A. De Mesmaeker, A. Waldner, V. Fritsch, R. M. Wolf, S. M. Freier, *Tetrahedron Lett.* **1993**, *34*, 6383–6386; b) A. De Mesmaeker, A. Waldner, J. Lebreton, P. Hoffmann, V. Fritsch, R. M. Wolf, S. M. Freier, *Synlett* **1993**, 733–736; c) A. De Mesmaeker, A. Waldner, J. Lebreton, P. Hoffmann, V. Fritsch, R. M. Wolf, S. M. Freier, *Angew. Chem. Int. Ed.* **1994**, *33*, 226–229; *Angew. Chem.* **1994**, *106*, 237–240; d) C. Selvam, S. Thomas, J. Abbott, S. D. Kennedy, E. Rozners, *Angew. Chem. Int. Ed.* **2011**, *50*, 2068–2070; *Angew. Chem.* **2011**, *123*, 2116–2118; e) P. Tanui, S. D. Kennedy, B. D. Lunstad, A. Haas, D. Leake, E. Rozners, *Org. Biomol. Chem.* **2014**, *12*, 1207–1210; f) D. Mutisya, C. Selvam, B. D. Lunstad, P. S. Pallan, A. Haas, D. Leake, M. Egli, E. Rozners, *Nucleic Acids Res.* **2014**, *42*, 6542–6551.
[8] a) Z. Huang, S. A. Benner, *J. Org. Chem.* **2002**, *67*, 3996–4013; b) B. Eschgfäller, J. G. Schmidt, M. König, S. A. Benner, *Helv. Chim. Acta* **2003**, *86*, 2959–2997.
[9] a) P. E. Nielsen, M. Egholm, R. H. Berg, O. Buchardt, *Science* **1991**, *254*, 1497–1500; b) Z. V. Zhilina, A. J. Ziemba, S. W. Ebbinghaus, *Curr. Top. Med. Chem.* **2005**, *5*, 1119–1131.
[10] a) S. K. Singh, A. A. Koshkin, J. Wengel, P. Nielsen, *Chem. Commun.* **1998**, 455–456; b) A. A. Koshkin, S. K. Singh, P. Nielsen, V. K. Rajwanshi, R. Kumar, M. Meldgaard, C. E. Olsen, J. Wengel, *Tetrahedron* **1998**, *54*, 3607–3630; c) J. S. Jepsen, M. D. Sörensen, J. Wengel, *Oligonucleotides* **2004**, *14*, 130–146.
[11] a) N. Papargyri, M. Pontoppidan, M. R. Andersen, T. Koch, P. H. Hagedorn, *Mol. Ther. Nucleic Acids.* **2020**, *19*, 706–717; b) A. Dieckmann, P. H. Hagedorn, Y. Burki, C. Brügmann, M. Berrera, M. Ebeling, T. Singer, F. Schuler, *Mol. Ther. Nucleic Acids* **2018**, *10*, 45–54.
[12] a) B. Schmidtgall, A. P. Spork, F. Wachowius, C. Höbartner, C. Ducho, *Chem. Commun.* **2014**, *50*, 13742–13745; b) B. Schmidtgall, C. Höbartner, C. Ducho, *Beilstein J. Org. Chem.* **2015**, *11*, 50–60.
[13] a) M. L. Jain, P. Y. Bruice, I. E. Szabó, T. C. Bruice, *Chem. Rev.* **2012**, *112*, 1284–1309; b) B. Schmidtgall, A. Kuepper, M. Meng, T. N. Grossmann, C. Ducho, *Chem. Eur. J.* **2018**, *24*, 1544–1553; c) M. Meng, C. Ducho, *Beilstein J. Org. Chem.* **2018**, *14*, 1293–1308.
[14] a) J. K. Strauss, C. Roberts, M. G. Nelson, C. Switzer, L. J. Maher III, *Proc. Natl. Acad. Sci. USA* **1996**, *93*, 9515–9520; b) T. P. Prakash, A. M. Kawasaki, E. A. Lesnik, N. Sioufi, M. Manoharan, *Tetrahedron* **2003**, *59*, 7413–7422; c) M. Prhavc, T. P. Prakash, G. Minasov, P. D. Cook, M. Egli, M. Manoharan, *Org. Lett.* **2003**, *5*, 2017–2020; d) S. Milton, D. Honcharenko, C. S. J. Rocha, P. M. D. Moreno, C. I. E. Smith, R. Strömberg, *Chem. Commun.* **2015**, ***51***, 4044–4047.
[15] a) G. Deglane, S. Abes, T. Michel, A. Laurent, M. Naval, C. Martinand-Mari, P. Prevot, E. Vives, I. Robbins, I. Barvik, Jr., B. Lebleu, F. Debart, J.-J. Vasseur, *Collection Symposium Series* **2005**, *7*, 143–147; b) G. Deglane, S. Abes, T. Michel, P. Prévot, E. Vives, F. Debrat, I. Barvik, B. Lebleu, J.-J. Vasseur, *ChemBioChem* **2006**, *7*, 684–692.
[16] R. L. Letsinger, C. N. Singman, G. Histand, M. Salunkhe, *J. Am. Chem. Soc.* **1988**, *110*, 4470–4471.
[17] a) A. Blasko, R. O. Dempcy, E. E. Minyat, T. C. Bruice, *J. Am. Chem. Soc.* **1996**, *118*, 7892–7899; b) D. A. Barawkar, T. C. Bruice, *Proc. Natl. Acad. Sci. USA* **1998**, *95*, 11047–11052; c) B. A. Linkletter, I. E. Szabo, T. C. Bruice, *J. Am. Chem. Soc.* **1999**, *121*, 3888–3896; d) H. Challa, T. C. Bruice, *Bioorg. Med. Chem. Lett.* **2001**, *11*, 2423–2427.
[18] a) D. P. Arya, T. C. Bruice, *J. Am. Chem. Soc.* **1998**, *120*, 6619–6620; b) H. Challa, T. C. Bruice, *Bioorg. Med. Chem. Lett.* **2001**, *11*, 2423–2427.
[19] M. Meng, B. Schmitdgall, C. Ducho, *Molecules* **2018**, *23*, 2941.
[20] a) L. A. McDonald, L. R. Barbieri, G. T. Carter, E. Lenoy, J. Lotvin, P. J. Petersen, M. M. Siegel, G. Singh, R. T. Williamson, *J. Am. Chem. Soc.* **2002**, *124*, 10260–10261; b) D. Wiegmann, S. Koppermann, M. Wirth, G. Niro, K. Leyerer, C. Ducho, *Beilstein J. Org. Chem.* **2016**, *12*, 769–795; c) T. Tanino, B. Al-Dabbagh, D. Mengin-Lecreulx, A. Bouhss, H. Oyama, S. Ichikawa, A. Matsuda, *J. Med. Chem.* **2011**, *54*, 8421–8439; d) A. P. Spork, M. Büschleb, O. Ries, D. Wiegmann, S. Boettcher, A. Mihalyi, T. D. H. Bugg, C. Ducho, *Chem. Eur. J.* **2014**, *20*, 15292–15297; e) S. Koppermann, Z. Cui, P. D. Fischer, X. Wang, J. Ludwig, J. S. Thorson, S. G. Van Lanen, C. Ducho, *ChemMedChem* **2018**, *13*, 779–784.
[21] C. I. E. Smith, R. Zain, *Annu. Rev. Pharmacol. Toxicol.* **2019**, *59*, 605–630.
[22] a) A. Matsuda, M. Satoh, T. Ueda, H. Machida, T. Sasaki, *Nucleosides Nucleotides* **1990**, *9*, 587–597; b) P. Herdewijn, J. Balzarini, M. Baba, R. Pauwels, A. Van Aerschot, G. Janssen, E. De Clercq, *J. Med. Chem.* **1988**, *31*, 2040–2048; c) S. Czernecki, J.-M. Valery, *Synthesis* **1991**, 239–240; d) R. Eisenhuth, C. Richert, *J. Org. Chem.* **2008**, *74*, 26–37.
[23] G. S. Ti, B. L. Gaffney, R. A. Jones, *J. Am. Chem. Soc.* **1982**, *104*, 1316–1319.
[24] A. M. Felix, E. P. Heimer, T. J. Lambros, C. Tzougraki, J. Meienhofer, *J. Org. Chem.* **1978**, *43*, 4194–4196.
[25] a) A. P. Spork, C. Ducho, *Org. Biomol. Chem.* **2010**, *8*, 2323–2326; b) A. P. Spork, D. Wiegmann, M. Granitzka, D. Stalke, C. Ducho, *J. Org. Chem.* **2011**, *76*, 10083–10098.
[26] a) J. Toulmé, *Nat. Biotechnol.* **2001**, *20*, 17; b) J. Kurreck, E. Wyszko, C. Gillen, V. A. Erdmann, *Nucleic Acids Res.* **2002**, *30*, 1911–1918.
[27] a) A. Novogrodsky, J. Hurwitz, *J. Biol. Chem.* **1966**, *241*, 2923–2932; b) C. C. Richardson, *Proc. Natl. Acad. Sci. USA* **1965**, *54*, 158–165; c) S. T. Crooke, K. M. Lemonidis, L. Neilson, R. Griffey, E. A. Lesnik, B. P. Monia, *Biochem. J.* **1995**, *312*, 599–608.
[28] C. Wahlestedt, P. Salmi, L. Good, J. Kela, T. Johnsson, T. Hökfelt, C. Broberger, F. Porreca, J. Lai, K. Ren, M. Ossipov, A. Koshkin, N. Jakobsen, J. Skouv, H. Henrik Oerum, M. H. Jacobsen, J. Wengel, *Proc. Natl. Acad. Sci. USA* **2000**, *97*, 5633–5638.
[29] X. Chi, P. Gatti, T. Papoian, *Drug Discovery Today* **2017**, *22*, 823–833.
[30] a) A. A. Koshkin, P. Nielsen, M. Meldgaard, V. K. Rajwanshi, S. K. Singh, J. Wengel, *J. Am. Chem. Soc.* **1998**, *120*, 13252–13253; b) K. Bondensgaard, M. Petersen, S. K. Singh, V. K. Rajwanshi, R. Kumar, J. Wengel, J. P. Jacobsen, *Chem. Eur. J.* **2000**, *6*, 2687–2695.

Manuscript received: July 8, 2020
Accepted manuscript online: July 13, 2020
Version of record online: August 28, 2020